Original Article

Check for updates

Available online at
www.heca-analitika.com/hjas

Heca Journal of Applied Sciences

Vol. 1, No. 2, 2023

Chemometric Classification Model for Assessing Chemical Composition Alterations in Patchouli Oil Post Zeolite Adsorption

Elly Sufriadi [1,2], Hesti Meilina[3], Agus Munawar [4], Abdelrahman O. Ezzat [5] and Rinaldi Idroes [6,*]

[1] Graduate School of Mathematics and Applied Sciences, Universitas Syiah Kuala, Banda Aceh 23111, Indonesia; elly.sufriadi@usk.ac.id (E.S.)
[2] Department of Chemistry, Faculty of Mathematics and Natural Sciences, Universitas Syiah Kuala, Banda Aceh 23111, Indonesia;
[3] Chemical Engineering Department, Faculty of Engineering, Universitas Syiah Kuala, Banda Aceh 23111, Indonesia; hesti.meilina@usk.ac.id (H.M.)
[4] Agricultural Technology Department, Universitas Syiah Kuala, Banda Aceh 23111, Indonesia; aamunawar@usk.ac.id (A.A.)
[5] Chemistry Department, College of Science, King Saud University, Riyadh 11451, Saudi Arabia; aezzat@ksu.edu.sa (A.O.E.)
[6] Department of Pharmacy, Faculty of Mathematics and Natural Sciences, Universitas Syiah Kuala, Banda Aceh 23111, Indonesia; rinaldi.idroes@usk.ac.id (R.I.)

* Correspondence: rinaldi.idroes@usk.ac.id

Article History

Received 6 August 2023
Revised 7 September 2023
Accepted 16 September 2023
Available Online 18 September 2023

Keywords:
Patchouli oil
Chemometrics
PLS-DA Classification
Zeolite
Absorption

Abstract

Various studies and applied processing by businesses have been done to improve the quality of Patchouli oil (PO), such as improving appearance, reducing heavy metal content, reducing acid numbers, and increasing the ratio of Patchouli alcohol (one of the active components of PO). However, this disregards the possibility of chemical composition change which will alter the original character of the PO. This study aims to identify the slightest shift in chemical composition from adding zeolite adsorbent into the PO. The classification model was built using Fourier transform infrared (FT-IR) spectra combined with chemometrics. The used FT-IR spectra for observation are 4000-500 cm-1 using Principal Component Analysis (PCA) and Partial Least Square-Discriminant Analysis (PLS-DA). The PO samples were from five points in Gayo Lues Regency, Province of Aceh, Indonesia, with PO added with zeolite at a ratio of 0.5%, 1.0%, 1.5%, 2.0%, and 2.5% (w/v) respectively. The classification model used in this study was able to classify between PO and PO added with zeolite at each level of the ratio. Prediction with deviation and Inlier vs. Hotelling's T^2 tests provide definitive information, with the results shown by the confusion matrix.

Copyright: © 2023 by the authors. This is an open-access article distributed under the terms of the Creative Commons Attribution-NonCommercial 4.0 International License. (https://creativecommons.org/licenses/by-nc/4.0/)

1. Introduction

Essential oils (EO) have existed thousands of years ago and have been used in various fields, especially for traditional medicine worldwide [1]. Currently, EO is a crucial commodity in the pharmaceutical industry, such as phytopharmaceuticals, drugs, cosmetics, body care, and the food and beverage industry. EO can be obtained from almost any plant, from flowers to tree roots. Among hundreds of EO, patchouli oil (PO) is one of the most widely known, especially in Asia such as China and India. Hundreds of years ago, China used PO in its medicine. In traditional Chinese medicine, PO has been used to reduce humidity, reduce the effects of summer and exterior syndrome, and be an antiemetic and appetite stimulant [2]. In traditional Indian medicine, the patchouli plant is used in the Ayurvedic, Unani, Sidda, and many other traditional ceremonies [3].

The patchouli plant was first described in 1845 by Pelletier-Sautelet and given the name *Pogestemon patchouli* [4]. PO producers include Indonesia, Vietnam, the Philippines, India, and China [5]. As one of the largest PO-producing countries globally, three patchouli species grow in Indonesia: *Pogostemon cablin* Benth, *Pogostemon hortensis* Benth, and *Pogostemon Heynanus* Benth [6]. Among the three species, *Pogostemon cablin* Benth is the most widely cultivated species for PO, especially in Aceh Province and other provinces on the Sumatra Island, Indonesia. The EO produced by *Pogostemon cablin* Benth is also used as an ingredient for fragrances and aromatherapy because of its dominant spicy aroma [7].

For decades, Indonesia has been the world's largest PO supplier, averaging 70% of the world's PO needs. Of the 70% of Indonesia's patchouli supply, 90% came from Aceh Province during the 80s [8]. Aceh Province is known to have high-quality PO and has always been a reference for PO quality in Indonesia [9] . The dominant regencies of PO producers are South Aceh and Gayo Lues. However, in the last ten years, PO production in Gayo Lues Regency has experienced a significant decline because most patchouli farmers have switched to citronella cultivation. The decline in PO production was also experienced by Aceh Province in general, shifting the biggest supplier of PO to Sulawesi Island.

In addition to a diminished production output, multiple indices pertaining to PO quality in Aceh exhibit heterogeneity across the various regencies of Aceh. The noted quality parameters of PO by exporters are the level of purity (free of water content), the level of heavy metal content such as iron and lead ions and, color and acid number. One cause of unstable oil quality is traditional refining facilities (kettles) where the reactor tube in the distillation still uses drums. The condenser pipe might also still use pipes made of iron with no boiler temperature control [10]. In addition to the production stage, the storage stage also contributes to the quality of patchouli oil. Another factor is the packaging; most farmers store oil in rustable metal cans, hence changing the oil color due to dissolved iron in the long run. Additionally, the oil stored in the collector of the distillation equipment is still mixed with water which clouds the oil [11]. The main components of PO are patchouli alcohol (PA) and norpatchoulenol. These two components give PO a distinctive aroma. Theoretically, the concentration of PA in patchouli oil is relatively higher (30-40%) compared to norpatchoulenol (0.3-0.4%). Superior quality patchouli oil must contain a high PA and the lowest terpene content possible. PO that meets the Indonesian National Standard (SNI 06-2385-2006) should have a minimum of 30% PA and a maximum acid number of 8 and is light yellow to reddish-brown [12], [13].

Various studies have been conducted to improve the quality of PO to increase product acceptability by importers. Zeolite adsorbents have been used to purify PO, characterized by a color change from dark brown to clear yellow. The use of zeolite can also reduce the acid number of the PO [14] [15] [16].

Unfortunately, these studies have not shown changes in PO's chemical composition despite the improvement of the quality process. Internationally, the ISO 3757 of 2002 (second edition, 2002-11-01) agreement stated that eight main components of PO must meet the minimum and maximum limits in percent units. It is estimated that any treatment to improve the quality of PO by adsorption process with zeolite will change the PO chemical composition [15]. Thus, it is necessary to research and observe changes in the chemical composition of PO and to assess other PO quality parameters.

In the present research, Principal Component Analysis (PCA) was instrumental in effectuating a reduction of multitudinous variables into a more concise set, while retaining a substantial proportion of the intrinsic variability diversity. Moreover, PCA adeptly transformed correlated original variables into novel, orthogonal counterparts [17, 18]. Historically, PCA has garnered widespread application across diverse disciplines, notably within intricate chemical and biological system analyses. The capability of PCA to distil extensive datasets into parsimonious and elucidative components positions it as an indispensable instrument within chemometrics. Furthermore, Partial Least Squares Discriminant Analysis (PLS-DA) holds potential in discerning among distinct varieties of essential oils predicated on their chemical profiles. This becomes exceedingly pivotal for essential oils derived from botanicals that present visual similarities, making them challenging to distinguish, exemplified by lavender and lavandin [19, 20]. Through PLS-DA, one can elucidate the provenance of the essential oil, ensuring its adherence to the requisite quality and specificity standards [21].

The purpose of this study is to assess changes in the PO chemical composition after zeolite adsorption using the FT-IR spectrum and chemometric analysis from five locations in Gayo Lues Regency, Aceh Province, Indonesia. Changes in composition were assessed on five variations of the mass of zeolite added to patchouli oil.

2. Materials and Methods

Patchouli oil samples of *Pogostemon cablin* Benth species were taken at five points in four sub-districts in Gayo Lues

Table 1. List of patchouli oil sample codes in Gayo Lues Regency.

Subdistricts	Village	Abbreviation	Coordinate	Altitude (masl)
Terangun	Terlis	POTr	4°00'58"N 96°57'28"E	1,455
		POTrZ-1	POTrZ added with zeolite at a ratio of 0.5% (b/V)	
		POTrZ -2	POTrZ added with zeolite at a ratio of 1.0% (b/V)	
		POTrZ -3	POTrZ added with zeolite at a ratio of 1.5% (b/V)	
		POTrZ -4	POTrZ added with zeolite at a ratio of 2.0% (b/V)	
		POTrZ -5	POTrZ added with zeolite at a ratio of 2.5% (b/V)	
	Persada Tongra	POTg	4°03'47"N 96°51'21"E	1,192
		POTgZ-1	POTg added with zeolite at a ratio of 0.5% (b/V)	
		POTgZ -2	POTg added with zeolite at a ratio of 1.0% (b/V)	
		POTgZ -3	POTg added with zeolite at a ratio of 1.5% (b/V)	
		POTgZ -4	POTg added with zeolite at a ratio of 2.0% (b/V)	
		POTgZ -5	POTg added with zeolite at a ratio of 2.5% (b/V)	
Blang Kejeren	Agusen	POA	3°54'18"N 97°23'02"E	1,095
		POAZ-1	POA added with zeolite at a ratio of 0.5% (b/V)	
		POAZ-2	POA added with zeolite at a ratio of 1.0% (b/V)	
		POAZ-3	POA added with zeolite at a ratio of 1.5% (b/V)	
		POAZ-4	POA added with zeolite at a ratio of 2.0% (b/V)	
		POAZ-5	POA added with zeolite at a ratio of 2.5% (b/V)	
Tripe Jaya	Perlak	POT	4°09'40"N 96°58'50"E	635
		POTZ-1	POT added with zeolite at a ratio of 0.5% (b/V)	
		POTZ-2	POT added with zeolite at a ratio of 1.0% (b/V)	
		POTZ-3	POT added with zeolite at a ratio of 1.5% (b/V)	
		POTZ-4	POT added with zeolite at a ratio of 2.0% (b/V)	
		POTZ-5	POT added with zeolite at a ratio of 2.5% (b/V)	
Blang Jerango	Ketukah	POK	4°03'35"N 97°08'10"E	710
		POKZ-1	POK added with zeolite at a ratio of 0.5% (b/V)	
		POKZ-2	POK added with zeolite at a ratio of 1.0% (b/V)	
		POKZ-3	POK added with zeolite at a ratio of 1.5% (b/V)	
		POKZ-4	POK added with zeolite at a ratio of 2.0% (b/V)	
		POKZ-5	POK added with zeolite at a ratio of 2.5% (b/V)	

Regency with varying geographic locations based on coordinates and altitude. Oil was purchased from oil refining facilities at each point. The distribution of sampling points in each district is shown in Table 1. The zeolite used is from Sigma-Aldrich CAS Number: 1318-02-1 and EC Number: 215-283-8.

The PO sampling location map is shown in Figure 1. PO samples from each location were divided into five vials with a volume of 10 ml each. Each vial was added with 0.5 g; 1.0 g; 1.5 g; 2.0 g; and 2.5 g of zeolite adsorbent to obtain PO with a ratio of 0.5% – 2.5% (w/v). The mixture was allowed to stand for 60 minutes, then filtered with Whatman filter grade GF/F circles, 47 mm, 100/pk. The filtered oil is then ready to be scanned with FT-IR.

2.1. ATR-FTIR Spectroscopy

The FTIR spectrum was obtained using the FTIR Shimadzu IR Model Prestige 21, Year 2012 (Japan) associated with ATR (attenuated total reflectance) sample media accessories with the reflection of one diamond crystal. The spectrum, in absorbance mode, was measured from 4000 cm^{-1} – 500 cm^{-1} with 25 scans of 4 cm^{-1} spectral resolution for PO from each location and five times for each zeolite addition ratio (% w/v). References (air background spectra) were scanned under the same instrumental conditions prior to each sample measurement. Spectra were processed with LabSolution IR Software version 3.2.0 spectroscopy software. A small drop of the PO sample is placed on the surface of the ATR diamond crystal for further sample spectra to be documented.

2.2. Chemometric Algorithms and Wavelength Range Selection

Classification is the process of categorizing data into distinct groups or classes [22–24]. The classification model is designed with two chemometrics approaches, namely unsupervised using PCA and Supervised using

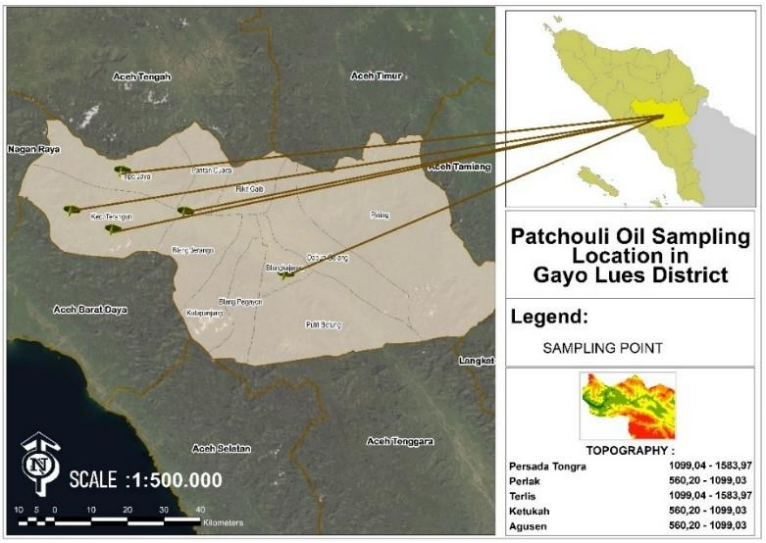

Figure 1. PO sampling location map.

PLS-DA [25]. In the PCA analysis, the Nonlinear Iterative Partial Least Squares (NIPALS) algorithm is used. This algorithm was chosen because it is numerically more accurate than the Singular-value Decomposition (SVD) algorithm, although it requires a longer computation time.In PCA analysis, the proper wavelength range is selected for analysis and produces a good separation. At the initial stage, the wavelength is 4000-400 cm^{-1}. Furthermore, because the distribution was very random, pre-processing was carried out with First Derivative and Standard Normal Variate (SNV), but it still did not give satisfactory grouping results. Based on these considerations, we analyzed the fingerprint area (1800-600 cm^{-1}), resulting in a satisfactory grouping. The test for selecting the wavelength range was carried out on samples from one point, namely Agussen, with the categories POA, POAZ1, POAZ2, POAZ3, POAZ4, and POAZ5 samples. The next model tested was to combine all PO samples from all points into one group and all POZ samples. Fixed grouping was done based on the ratio of zeolite to patchouli oil with a code; PO, POZ1, POZ2, POZ3, POZ4, POZ5. The result showed a separation between the various points of the PO sample and an overlap between the PO sample and the POZ sample. Thus, the further analysis used a separate analysis for each sample point and was done in the wavelength range of 1800-600 cm^{-1}.

PLS is a classic method in chemometrics analysis that can improve the covariance between latent variables and responses [26]. PLS has been widely applied in chemometrics, including in the use of spectral data. There are several PLS algorithms, including NIPALS and SIMPLS. These two types differ in computational complexity and numerical stability. The computing time is influenced by the data dimensions and the number of predetermined latent variables [27]. Numerical stability depends on the numerical calculation method used and is a factor of model precision. Theoretically, all PLS algorithms should produce the same model; in practice, there are differences due to numerical calculation methods. In this study, the algorithm used is Kernel PLS because it could build a non-linear regression model that could handle high-dimensional data [28].

Validation was done using the PO dataset, which was scanned on different days. The PCA and PLS-DA analysis process uses Unscrambler X software version 10.46, released by Camo Software in 2016. Data validation in this classification model was done by taking five spectra of ATR-FTIR measurement results on different days, both for PO and POZ, resulting in 10 obtained datasets for validation.

3. Results and Discussion

3.1. ATR-FTIR Spectrometry

The characteristic infrared spectra for pure patchouli oil (PO) and zeolite-added patchouli oil (POZ) are shown in Figure 2. These spectra look similar to the typical characteristic of absorption peaks for common triglycerides. Additionally, all are present with terpenoid compounds. Visually, there is no significant difference in peaks for the six spectra. A common indication for such symptoms is that the main functional groups of the PO components do not change. However, in more detail, a more rigorous investigation with a different approach is needed. Therefore, it is necessary to experiment with multivariate analysis, both unsupervised and supervised [29].

Ordinary FTIR spectra are complicated due to overlapping spectra of individual components and the

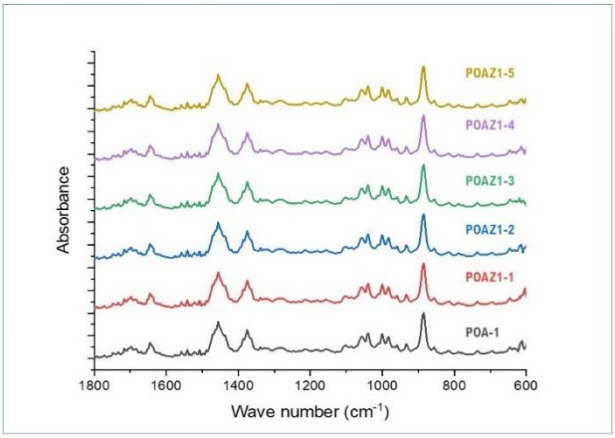

Figure 2. Comparison of FTIR spectrum between POA and POAZ. Note: POA-1: PO from Agussen; POAZ: POA with added zeolite; POAZ-1 (0.5%); POAZ-2 (1.0%); POAZ-3 (1.5%): POAZ-4 (2.0%); and POAZ-5 (2.5%) (w/v)

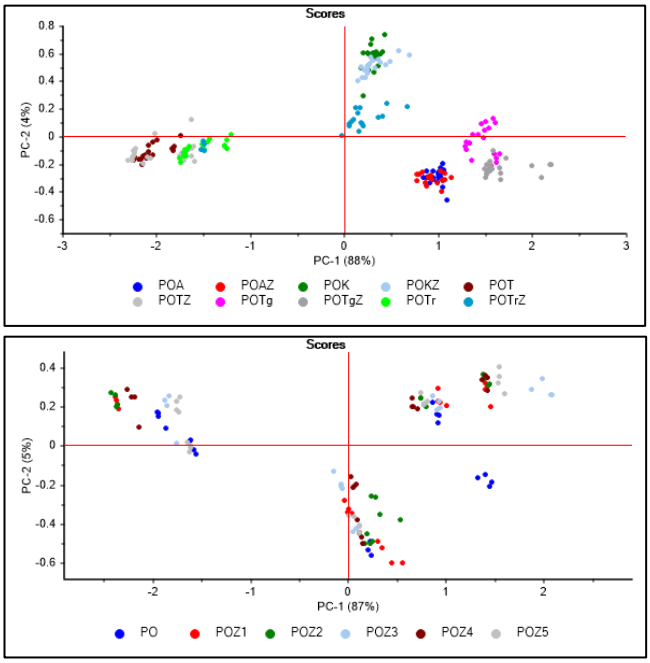

Figure 3. Testing of the spectra-combined sample locations model

mixing of different vibration modes, despite the main component contribution never exceeding 25% [30]. Of the total content, the compounds in PO that occur at low concentrations (<1%) did not significantly affect the ATR-FTIR spectra. The ATR-FTIR spectra from PO samples present characteristics of spectral fingerprints and can be used to compare different plant species and chemotypes [25].

3.2. Principal Component Analysis (PCA)

The preliminary analysis to select the wavelength range and the sample grouping model showed the 4000-400 cm^{-1} wavelength range produced a score plot displaying a dispersed PO and POZ and not clustered. Visually, the same appearance occurs in the score plot of the pre-processing first derivative and standard normal variate (SNV) results, as shown in Figure 3. With these considerations, the subsequent stage of testing is carried out on the fingerprint area, 1800-600 cm^{-1}[31][32].

PO separation from these five locations could be due to differences in age at harvest and altitude cultivation, as shown in Table 1. However, this study did not study the effect of patchouli plant planting locations and harvest age and disregarded those factors [33].

Based on the preliminary test, a separate analysis was conducted for each location using the same model. The result showed that the five locations displayed the same separation pattern between PO and POZ, as shown in Figure 5 [34].

The Principal Component Analysis is a method to reduce a complex data set into a smaller set of latent variables, known as principal components (PC) [18, 25, 35]. With many spectral bands (input variables), interpreting the data in a meaningful way can be done by reducing the number of variables to some linear combination of spectral bands that can be easily explained. The first two PCs capture most of the information and are sufficient to illustrate the gist of the data in the PCA correlation matrix, as evidenced by the steep lines that bend quickly and then flatten [32]. Here, treatment was conducted to identify a difference between the PO and POZ spectra input and validated with the PO and POZ datasets at various mixing ratios between PO and zeolite. From the five test points of PO samples, the same symptom was obtained in PO added with zeolite; differences occurred due to a change in chemical composition, either reduced, increased, or completely disappeared (Figure 5) [31, 36, 37].

The visualization in Figure 4 shows that the distribution between the data points of the training set and the test set (validation) has similarities in the grouping. This illustrates that ATR-FTIR can detect PO without the zeolite addition despite it being in the unsupervised category (PCA analysis) [29, 38, 39]. This visualization also shows that differences between PO and PO added with zeolite are seen in all sample locations, although there are differences in altitude cultivation. An interesting finding from the loading plot for each sample location was that differences in the wavelength range affect the response to PCA analysis [18, 35]. The difference in the wavelength range indicates different compound functional groups. The addition of zeolite can have a different impact on the chemical composition of PO, as evidenced by examining the loading plot of the five sample locations in Figure 5 [40, 41].

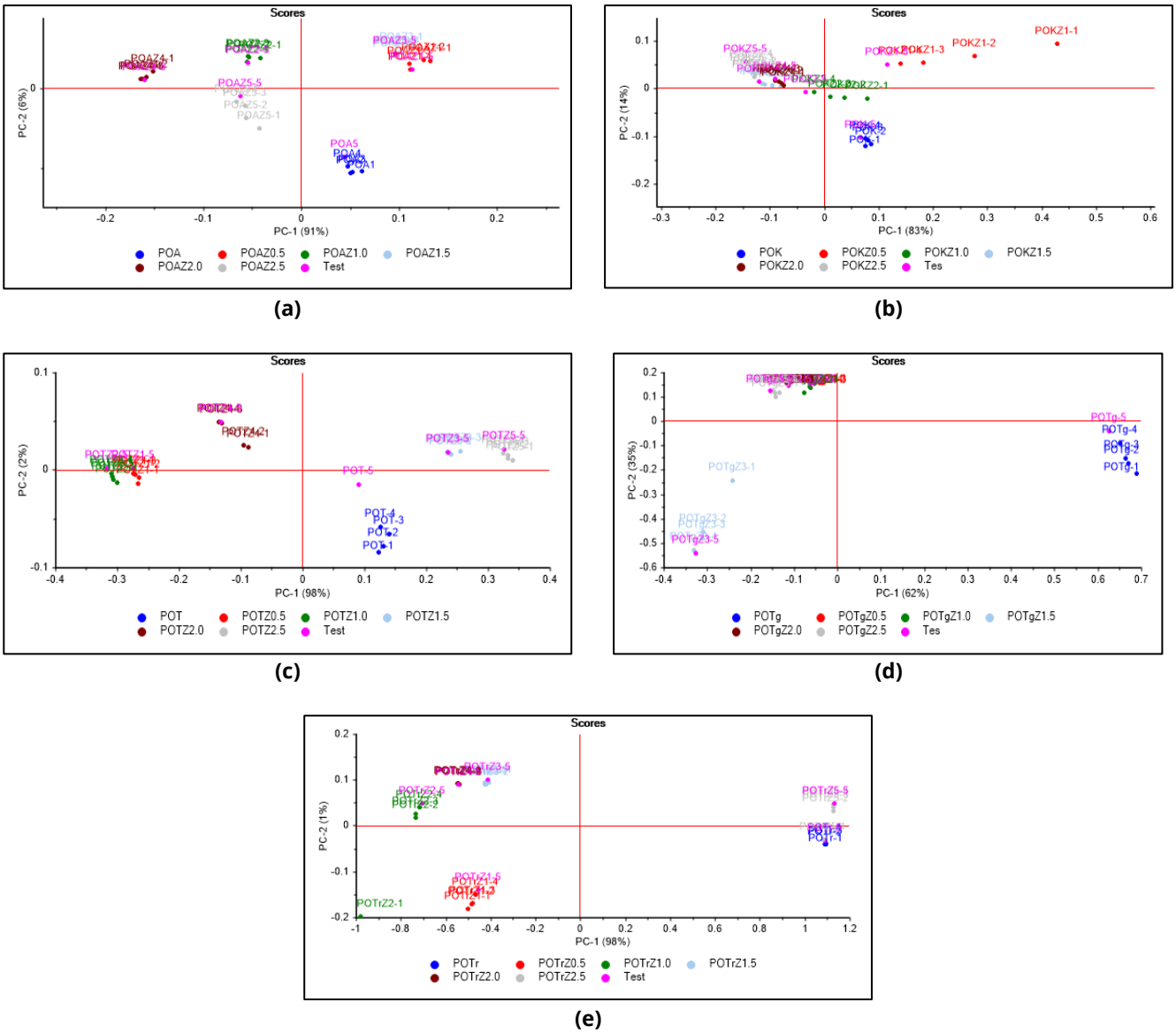

Figure 4. PCA Score plot of PO and POZ from 5 locations in Gayo Lues.

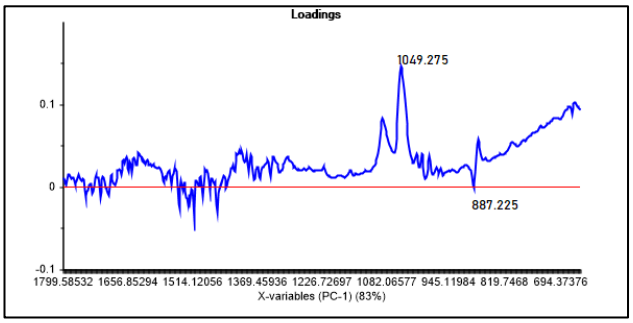

Figure 5. PCA Loading plot of PO and POZ from 5 locations in Gayo Lues

Figure 5 indicates that the PO from Agussen (A) shows changes in chemical composition that occur in chemical components with C=C-H groups and Ar-H bonds, namely groups with wavelengths between 1000-650 cm^{-1}. The PO of Tapah (B) is predicted to experience a chemical composition change with similar groups to A because the curve shows the lowest peak is at wavelengths of 887 cm^{-1} [37, 42]. Another group that experienced changes in chemical composition was seen in PO from Perlak Tripe Jaya (C), with changes occurring in the wavelength range of 1539-1527 cm^{-1}, indicating the presence of aromatic and aliphatic C=C groups and C=N bonds. The same thing happened to PO from Terlis (D) and Tongra (E). However, the results shown by PCA analysts need to be confirmed by classifying with PLS-DA [27, 42].

3.3. Partial Least Square-Discriminant Analysis (PLS-DA)

The PLS-DA method is derived from the PLS method, which is used to perform regression. PLS can model the relationship between the observed dataset variables and the latent vector (score/component vector), given by the two observed dataset variables, where X = [xi,..., xn] ε R^N

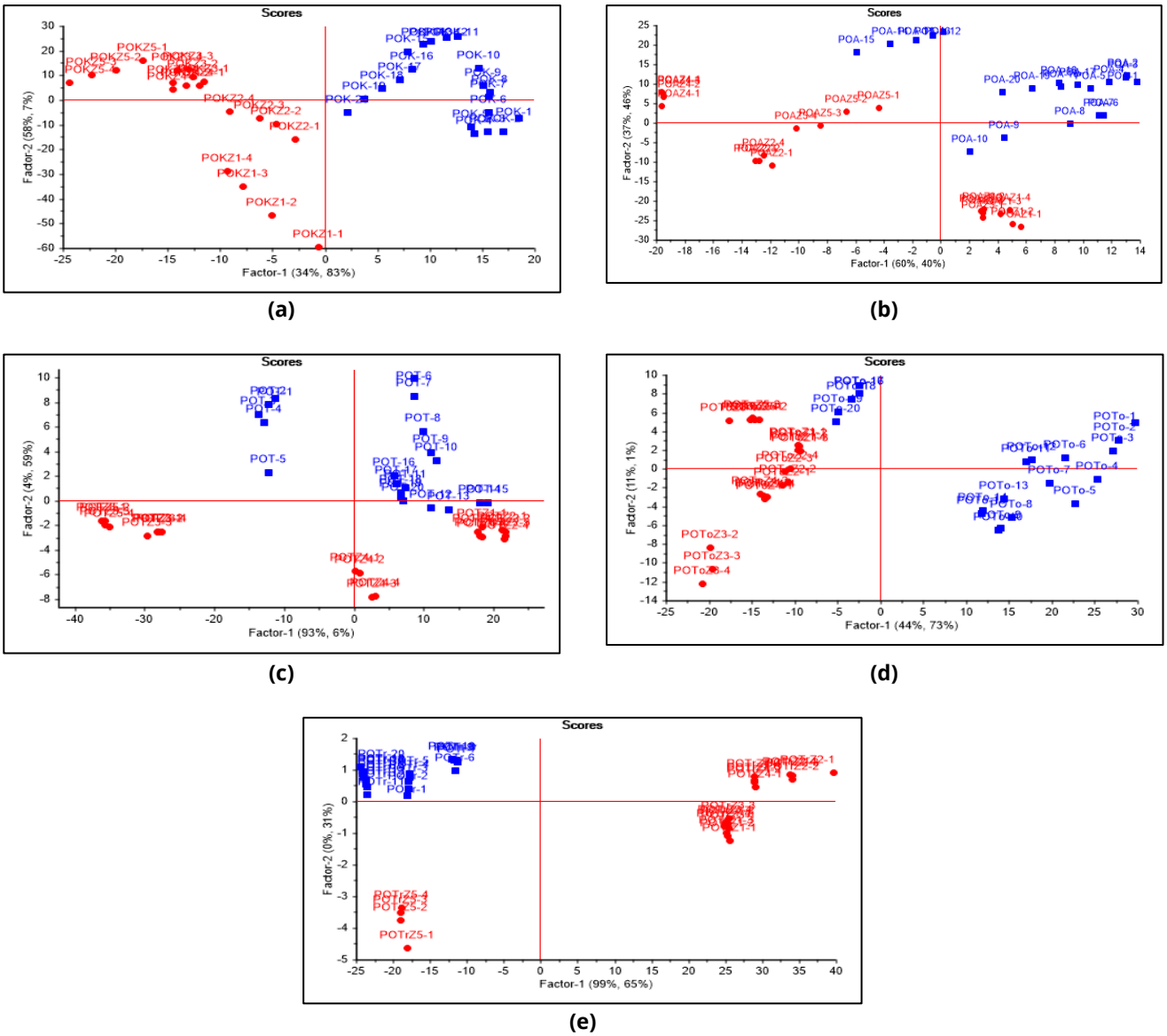

Figure 6. Score plot for PLS against PO and POZ from five locations.

and Y = [yi,..., yn] ε R^N, where X and Y are the central mean. PLS decomposes X and Y into: X = TP^T + E and Y = UQ^T+ F[43]. Classification by PLS-DA on the data set consisting of PO and PO mixed with zeolite at a ratio of 0.5-2.5% (w/v) obtained a score plot as shown in Figure 6 [33, 38, 44, 45].

Figure 7 shows the clear separation pattern between PO and POZ, confirming the separation in the previous PCA analysis. In addition, the loading plot result indicates a change in the chemical compounds with functional groups in the wavelengths of 885-871 cm^{-1}; on PCA, it is shown at 886-871 cm^{-1}[43]. In addition, among the four factors in the analysis, the classification results are the same between calibration and validation in factor 2.

Each PLS-DA model was assessed repeatedly through six v-fold variants, namely: cross-validation (CV), v (v = 2, 4, 5, 7, 10, 15), auto prediction (AP) and external testing (ET). For the POA above, the separation of the training set and the test set in ET and CV has been conducted in an adjusted manner, ensuring all subsets of the original dataset contain a similar proportion of classes [46]. External testing, on the other hand, each of the four data subsets was separated independently via the PLS Kernel algorithm at a ratio of 7:3. By applying sampling to the entire dataset, the procedure was carried out independently on 40 different data subsets defined by the model. (i.e., PLS Kernel algorithm). Training sets and test sets of 50 data subsets were collected [27, 47, 48]. Predicted results from the three locations indicate that the model provides information that confirms a change in chemical composition from zeolite addition. The deviation value is relatively low based on the classification model proposed in the PLS-DA analysis (Figure 7).

Table 2. Distribution of calibration and validation values of PLS-DA analysis results for the five samples

		Slope	Offset	RMSE	R-Square
POA	Calibration	0.9882667	5.7817E-07	0.10832	0.9882668
	Validation	0.9712065	-0.0014934	0.154255	0.9773803
POK	Calibration	0.9853219	1.7881E-07	0.1211562	0.9853212
	Validation	0.9806675	-0.0073358	0.1853493	0.9673419
POT	Calibration	0.9456055	-3.4049E-07	0.2332254	0.9456059
	Validation	0.9277973	-0.0023715	0.289726	0.9202034
POTg	Calibration	0.8855736	1.5609E-07	0.3382708	0.8855729
	Validation	0.0117161	0.0117161	0.4166252	0.8349937
POTr	Calibration	0.9749908	-6.1095E-08	0.1581425	0.9749909
	Validation	0.9653341	0.0016365	0.17837	0.969755

Table 3. Shifts of the confusion matrix between PO and POZ on Augussen samples.

Predicted	Actual	A	B	E	F
A	1	20	0	0	0
B	2	0	11	0	1
E	3	0	0	5	0
F	4	0	9	0	4

Note: A: Group for PO training set
B: Group for PO training set Z
E and F: Test-set for PO and POZ

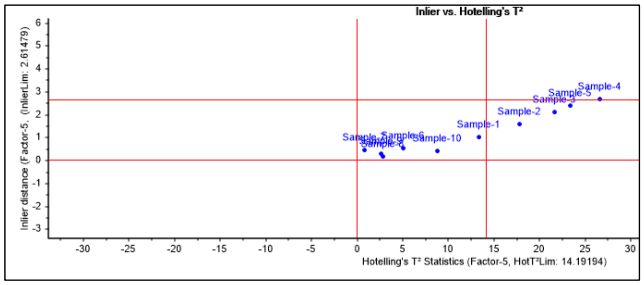

Figure 7. Prediction regression for unknown samples.

To ensure the predictions are reliable, it needs to be proven by analyzing the relationship between Inlier vs. Hotelling's T^2 parameter. The predicted sample should not be too far from the calibration sample, checked by the Inlier distance. The sample projection in the model should also not be too far from the center, checked with the T^2 Hotelling distance [49]. The calibration and validation samples are not too far apart and even centered in a quadrant in the middle. This model is tested again by making predictions from the PLS results on the validation data, which shows a significant separation between PO and POZ, as shown in Figure 8.

Table 2 presents the root mean square errors (RMSE), indicating their low values, which are close to 0. These results affirm the appropriateness of the classification model. Table 3 provides a comparison between calibration and validation values. In general, the R square values are very close between calibration and validation, with most approaching 1, except for POTg, which remains below 0.9.

In addition to using the above approach, paying attention to the confusion matrix is also necessary. When building a classification model with machine learning, how to get the best model is always questioned. In this case, it is essential to measure the performance of the model built from machine learning to ensure it is considered in choosing the "best" model. The confusion matrix is used to measure the model's performance, especially for classification (supervised learning) in machine learning. The test on one sample obtained two crucial pieces of information: provide certainty that the model used is correct and provide information that when zeolite changes in PO, ATR-FTIR combined with chemometrics can detect the addition of zeolite as shown in Table 3. The table shows that none of the 20 PO training data sets grouped as A shifted to group B, while 11 of the 20 training data sets grouped as B shifted to group F. Furthermore, 5 PO spectra used as validation (E) also remained in group E and none of them shifted to group F.

4. Conclusions

The FTIR spectra data analyzed by chemometrics can detect the presence of zeolite addition in low, medium, and high ratios. The presence of 0.5% (w/v) of visible zeolite can be readily identified, both by unsupervised analyzes such as PCA and by supervised analysis (PLS-DA). The same symptoms were also seen in the highest zeolite ratio, 2.5% (w/v). The classification model proposed in this study is quite promising after testing with the PLS-DA approach, especially after observing the

predicted with deviation and Inlier vs. Hotelling's T2 and the confusion matrix.

Author Contributions: Conceptualization, E.E. and R.I.; methodology, A.M.; software, H.M. and A.E.O.; validation, E.S. and A.M.; formal analysis, H.M..; investigation, E.S..; resources, R.I.; data curation, A.M.; writing—original draft preparation, E.S.; writing—review and editing, A.M. and R.I.; visualization, H.M and A.O.E.; supervision, R.I.; project administration, E.S.; funding acquisition, R.I. All authors have read and agreed to the published version of the manuscript.

Funding: PMBKM Research Grant Fiscal Year 2023, Number: 356/UN11.2.1/PT.01.03/PNBP/2023 dated May 3, 2023, this project is funded by Syiah Kuala University, The Ministry of Education, Culture, Research, and Technology.

Ethical Clearance: Not applicable.

Informed Consent Statement: Not applicable.

Data Availability Statement: All datasets generated and analyzed during the current study are available in the Dataset repository. Data not publicly available due to specific reason, e.g., containing information that could compromise the privacy of research participants, proprietary restrictions, etc. It can be made available from the corresponding author upon reasonable request and subject to appropriate confidentiality agreements.

Acknowledgments: The authors of this study express their gratitude to the Ministry of Education and Culture of Research and Technology for providing funding through the PMBKM Research Grant Fiscal Year 2023, Number: 356/UN11.2.1/PT.01.03/PNBP/2023 dated May 3, 2023, this project is funded by Syiah Kuala University. This support has been instrumental in enabling the authors to carry out this research endeavor. The authors acknowledge the contributions of all those who have assisted in the implementation of this study, including colleagues, supervisors, technical staff, and any other individuals who have supported this work in various capacities. Their invaluable contributions have been fundamental to the successful completion of this research. The authors would also like to extend their thanks to all participants who have willingly participated in this study. Their cooperation and participation have been integral to the validity and reliability of the results obtained.

Conflicts of Interest: There are no conflicts to declare.

References

1. Movahhed Haghighi, T., Saharkhiz, M. J., Khosravi, A. R., Raouf Fard, F., and Moein, M. (2017). Essential oil content and composition of Vitex pseudo-negundo in Iran varies with ecotype and plant organ, *Industrial Crops and Products*, Vol. 109, No. August, 53–59. doi:10.1016/j.indcrop.2017.08.007.
2. Wu, J., Gan, Y., Li, M., Chen, L., Liang, J., Zhuo, J., Luo, H., Xu, N., Wu, X., Wu, Q., Lin, Z., Su, Z., and Liu, Y. (2020). Patchouli alcohol attenuates 5-fluorouracil-induced intestinal mucositis via TLR2/MyD88/NF-kB pathway and regulation of microbiota, *Biomedicine and Pharmacotherapy*, Vol. 124, No. January, 109883. doi:10.1016/j.biopha.2020.109883.
3. Swamy, M., and Sinniah, U. (2015). A Comprehensive Review on the Phytochemical Constituents and Pharmacological Activities of Pogostemon cablin Benth.: An Aromatic Medicinal Plant of Industrial Importance, *Molecules*, Vol. 20, No. 5, 8521–8547. doi:10.3390/molecules20058521.
4. Swamy, M. K., and Sinniah, U. R. (2016). Patchouli (Pogostemon cablin Benth.): Botany, agrotechnology and biotechnological aspects, *Industrial Crops and Products*, Vol. 87, 161–176. doi:10.1016/j.indcrop.2016.04.032.
5. Sufriadi, E., Aisyah, Y., Harahap, F., Fernando, Y., and Mardina, V. (2020). A method for aseptic culture of bud explants pogestemon cablin benth Var Tapak Tuan, Aceh, Indonesia, *IOP Conference Series: Materials Science and Engineering*, Vol. 725, No. 1. doi:10.1088/1757-899X/725/1/012066.
6. Halimursyadah, Syamsuddin, Nurhayati, Zuliana, and Phonna, T. N. (2021). Interaction between type of plant growth promoting rhizobacteria and patchouli varieties on growth and yield of patchouli (Pogostemon cablin Benth.), *IOP Conference Series: Earth and Environmental Science*, Vol. 667, No. 1. doi:10.1088/1755-1315/667/1/012073.
7. Dantas, T. N. C., Cabral, T. J. O., Dantas Neto, A. A., and Moura, M. C. P. A. (2020). Enrichmnent of patchoulol extracted from patchouli (Pogostemon cablin) oil by molecular distillation using response surface and artificial neural network models, *Journal of Industrial and Engineering Chemistry*, Vol. 81, 219–227. doi:10.1016/j.jiec.2019.09.011.
8. Cano-Reinoso, D. M., Purwanto, Y. A., Budiastra, I. W., Sutrisno, Kuroki, S., Widodo, S., and Kamanga, B. M. (2021). Determination of α-guaiene and azulene chemical content in patchouli aromatic oil (Pogostemon cablin benth.) from indonesia by near-infrared spectroscopy, *Indian Journal of Natural Products and Resources*, Vol. 12, No. 2, 256–262. doi:10.56042/ijnpr.v12i2.24657.
9. Sufriadi, E., Idroes, R., Meilina, H., Munawar, A. A., Lelifajri, N., and Indrayanto, G. (2023). Partial Least Squares-Discriminant Analysis Classification for Patchouli Oil Adulteration Detection by Fourier Transform Infrared Spectroscopy in Combination with Chemometrics, *ACS Omega*. doi:10.1021/acsomega.3c00080.
10. Sufriadi, E., Meilina, H., Munawar, A. A., Muhammad, S., and Idroes, R. (2021). Identification of β-Caryophyllene (BCP) in Aceh patchouli essential oil (PEO) using gas chromatography-mass pectrophotometry (GC-MS), *IOP Conference Series: Earth and Environmental Science* (Vol. 667), IOP Publishing, 12032.
11. Sufriadi, E., Meilina, H., Munawar, A. A., and Idroes, R. (2021). Fourier Transformed Infrared (FTIR) spectroscopy analysis of patchouli essential oils based on different geographical area in Aceh, *IOP Conference Series: Materials Science and Engineering*, Vol. 1087, No. 1, 012067. doi:10.1088/1757-899X/1087/1/012067.
12. Kusuma, H. S., Altway, A., and Mahfud, M. (2018). Solvent-free microwave extraction of essential oil from dried patchouli (Pogostemon cablin Benth) leaves, *Journal of Industrial and Engineering Chemistry*, Vol. 58, 343–348. doi:10.1016/j.jiec.2017.09.047.
13. Kimia, J. T., Teknik, F., and Kuala, U. S. (2007). Aplikasi Proses Pengkelatan untuk Peningkatan Mutu Minyak Nilam Aceh, *Jurnal Rekayasa Kimia & Lingkungan*, Vol. 6, No. 2, 63–66.
14. Hardyanti, I. S., Septyaningsih, D., Nurani, I., Agus, E., and Wibowo, P. (2016). Analisis Kadar Patchouli Alcohol menggunakan Gas Chromatography pada Pemurnian Minyak Nilam menggunakan Adsorben Zeolit, *Prosiding Seminar Nasional XI "Rekayasa Teknologi Industri Dan Informasi 2016 Sekolah Tinggi Teknologi Nasional Yogyakarta*, 392–395.
15. Sri Hardyanti, I., Nurkhalisa, S., and Maghfiroh, H. (2017). Comparison of bentonite and zeolite as adsorbent purification process of patchouli oil (Pogostemon cablin), *Journal of Scientific and Innovative Research*, Vol. 6, No. 2, 87–90.
16. Wijaya, K., Utami, M., Syoufian, A., and Murifal, A. I. (2021). Solid State Mixing Preparation of CaO/Bentonite Nanocomposite and its Application to Improve the Quality of Patchouli Oil, *Materials*

and Technologies for Engineering Application (Vol. 1162), Trans Tech Publications Ltd, 21–26. doi:10.4028/www.scientific.net/AMR.1162.21.

17. Suhandy, D., and Yulia, M. (2021). Classification of lampung robusta Specialty coffee according to differences in cherry processing methods using UV spectroscopy and chemometrics, *Agriculture (Switzerland)*, Vol. 11, No. 2, 1–11. doi:10.3390/agriculture11020109.

18. Arslan, F. N., Akin, G., Karuk Elmas, Ş. N., Yilmaz, I., Janssen, H. G., and Kenar, A. (2019). Rapid detection of authenticity and adulteration of cold pressed black cumin seed oil: A comparative study of ATR–FTIR spectroscopy and synchronous fluorescence with multivariate data analysis, *Food Control*, Vol. 98, No. December 2018, 323–332. doi:10.1016/j.foodcont.2018.11.055.

19. de Girolamo, A., Cervellieri, S., Mancini, E., Pascale, M., Logrieco, A. F., and Lippolis, V. (2020). Rapid authentication of 100% Italian durum wheat pasta by FT-NIR spectroscopy combined with chemometric tools, *Foods*, Vol. 9, No. 11. doi:10.3390/foods9111551.

20. Tarhan, İ., Bakır, M. R., Kalkan, O., Yöntem, M., and Kara, H. (2022). Rapid determination of adulteration of clove essential oil with benzyl alcohol and ethyl acetate: Towards quality control analysis by FTIR with chemometrics, *Vibrational Spectroscopy*, Vol. 118, No. December 2021, 1–10. doi:10.1016/j.vibspec.2022.103339.

21. Lafhal, S., Vanloot, P., Bombarda, I., Kister, J., and Dupuy, N. (2016). Chemometric analysis of French lavender and lavandin essential oils by near infrared spectroscopy, *Industrial Crops and Products*, Vol. 80, 156–164. doi:10.1016/j.indcrop.2015.11.017.

22. Noviandy, T. R., Maulana, A., Idroes, G. M., Maulydia, N. B., Patwekar, M., Suhendra, R., and Idroes, R. (2023). Integrating Genetic Algorithm and LightGBM for QSAR Modeling of Acetylcholinesterase Inhibitors in Alzheimer's Disease Drug Discovery, *Malacca Pharmaceutics*, Vol. 1, No. 2, 48–54. doi:10.60084/mp.v1i2.60.

23. Maulana, A., Faisal, F. R., Noviandy, T. R., Rizkia, T., Idroes, G. M., Tallei, T. E., El-Shazly, M., and Idroes, R. (2023). Machine Learning Approach for Diabetes Detection Using Fine-Tuned XGBoost Algorithm, *Infolitika Journal of Data Science*, Vol. 1, No. 1, 1–7. doi:10.60084/ijds.v1i1.72.

24. Noviandy, T. R., Maulana, A., Emran, T. B., Idroes, G. M., and Idroes, R. (2023). QSAR Classification of Beta-Secretase 1 Inhibitor Activity in Alzheimer's Disease Using Ensemble Machine Learning Algorithms, *Heca Journal of Applied Sciences*, Vol. 1, No. 1, 1–7. doi:10.60084/hjas.v1i1.12.

25. Agatonovic-Kustrin, S., Ristivojevic, P., Gegechkori, V., Litvinova, T. M., and Morton, D. W. (2020). Essential oil quality and purity evaluation via ft-ir spectroscopy and pattern recognition techniques, *Applied Sciences (Switzerland)*, Vol. 10, No. 20, 1–12. doi:10.3390/app10207294.

26. Wulandari, L., Idroes, R., Noviandy, T. R., and Indrayanto, G. (2022). Application of chemometrics using direct spectroscopic methods as a QC tool in pharmaceutical industry and their validation, 327–379. doi:10.1016/bs.podrm.2021.10.006.

27. Song, W., Wang, H., Maguire, P., and Nibouche, O. (2018). Nearest clusters based partial least squares discriminant analysis for the classification of spectral data, *Analytica Chimica Acta*, Vol. 1009, 27–38. doi:10.1016/j.aca.2018.01.023.

28. Rosipal, R., and Trejo, L. J. (2000). 10.1162/15324430260185556, *CrossRef Listing of Deleted DOIs*, Vol. 1, 97–123. doi:10.1162/15324430260185556.

29. Bombarda, I., Dupuy, N., Da, J. P. L. Van, and Gaydou, E. M. (2008). Comparative chemometric analyses of geographic origins and compositions of lavandin var. Grosso essential oils by mid infrared spectroscopy and gas chromatography, *Analytica Chimica Acta*, Vol. 613, No. 1, 31–39. doi:10.1016/j.aca.2008.02.038.

30. da Costa, N. L., da Costa, M. S., and Barbosa, R. (2021). A Review on the Application of Chemometrics and Machine Learning Algorithms to Evaluate Beer Authentication, *Food Analytical Methods*, Vol. 14, No. 1, 136–155. doi:10.1007/s12161-020-01864-7.

31. Martins, J. P. A., Teófilo, R. F., and Ferreira, M. M. C. (2010). Computational performance and cross-validation error precision of five PLS algorithms using designed and real data sets, *Journal of Chemometrics*, Vol. 24, No. 6, 320–332. doi:10.1002/cem.1309.

32. Zhao, H., and Ji, S. (2018). Near Infrared Spectroscopy Evaluation and Regional Analysis of Chinese Pogostemon cablin and Agastache rugosa, Vol. 8, No. 1, 1–12.

33. Lee, L. C., Liong, C. Y., and Jemain, A. A. (2018). Partial least squares-discriminant analysis (PLS-DA) for classification of high-dimensional (HD) data: A review of contemporary practice strategies and knowledge gaps, *Analyst*, Vol. 143, No. 15, 3526–3539. doi:10.1039/c8an00599k.

34. Katerinopoulou, K., Kontogeorgos, A., Salmas, C. E., Patakas, A., and Ladavos, A. (2020). Geographical origin authentication of agri-food products: A review, *Foods*, Vol. 9, No. 4, 1–16. doi:10.3390/foods9040489.

35. Diego, M. C. R., Purwanto, Y. A., Sutrisno, S., and Budiastra, I. W. (2018). Determination of the Characteristics and Classification of Near-Infrared Spectra of Patchouli Oil (Pogostemon Cablin Benth.) from Different Origin, *IOP Conference Series: Earth and Environmental Science*, Vol. 147, No. 1. doi:10.1088/1755-1315/147/1/012013.

36. Gomes, M. V. da S., da Silva, J. D., Ribeiro, A. F., Cabral, L. M., and de Sousa, V. P. (2019). Development and validation of a quantification method for α-humulene and trans-caryophyllene in Cordia verbenacea by high performance liquid chromatography, *Revista Brasileira de Farmacognosia*, Vol. 29, No. 2, 182–190. doi:10.1016/j.bjp.2019.01.009.

37. Fahmi, Z., Mudasir, and Rohman, A. (2020). Attenuated total reflectance-FTIR spectra combined with multivariate calibration and discrimination analysis for analysis of patchouli oil adulteration, *Indonesian Journal of Chemistry*, Vol. 20, No. 1, 1–8. doi:10.22146/ijc.36955.

38. Lee, L. C., and Jemain, A. A. (2019). Predictive modelling of colossal ATR-FTIR spectral data using PLS-DA: Empirical differences between PLS1-DA and PLS2-DA algorithms, *Analyst*, Vol. 144, No. 8, 2670–2678. doi:10.1039/c8an02074d.

39. Rohman, A., and Man, Y. B. C. (2010). Fourier transform infrared (FTIR) spectroscopy for analysis of extra virgin olive oil adulterated with palm oil, *Food Research International*, Vol. 43, No. 3, 886–892. doi:10.1016/j.foodres.2009.12.006.

40. Adinew, B. (2014). GC-MS and FT-IR analysis of constituents of essential oil from Cinnamon bark growing in South-west of Ethiopia, *International Journal of Herbal Medicine*, Vol. 1, No. 6, 22–31.

41. Silva-Filho, S. E., Wiirzler, L. A. M., Cavalcante, H. A. O., Uchida, N. S., de Souza Silva-Comar, F. M., Cardia, G. F. E., da Silva, E. L., Aguiar, R. P., Bersani-Amado, C. A., and Cuman, R. K. N. (2016). Effect of patchouli (Pogostemon cablin) essential oil on in vitro and in vivo leukocytes behavior in acute inflammatory response, *Biomedicine and Pharmacotherapy*, Vol. 84, 1697–1704. doi:10.1016/j.biopha.2016.10.084.

42. Hzounda, J. B. F., Jazet, P. M. D., Lazar, G., Răducanu, D., Caraman, I., Bassene, E., Boyom, F. F., and Lazar, I. M. (2016). Spectral and chemometric analyses reveal antioxidant properties of essential oils from four Cameroonian Ocimum, *Industrial Crops and Products*, Vol. 80, 101–108. doi:10.1016/j.indcrop.2015.09.077.

43. Aminu, M., and Ahmad, N. A. (2020). Complex Chemical Data Classification and Discrimination Using Locality Preserving Partial Least Squares Discriminant Analysis, *ACS Omega*, Vol. 5, No. 41, 26601–26610. doi:10.1021/acsomega.0c03362.

44. Tan, C. S., Leow, S. Y., Ying, C., Tan, C. J., Yoon, T. L., Jingying, C., and Yam, M. F. (2021). Comparison of FTIR spectrum with chemometric and machine learning classifying analysis for differentiating guan-mutong a nephrotoxic and carcinogenic traditional chinese medicine with chuan-mutong, *Microchemical Journal*, Vol. 163, No. December 2020, 105835. doi:10.1016/j.microc.2020.105835.

45. Ruiz-Perez, D., Guan, H., Madhivanan, P., Mathee, K., and Narasimhan, G. (2020). So you think you can PLS-DA?, *BMC Bioinformatics*, Vol. 21, No. Suppl 1, 1–10. doi:10.1186/s12859-019-3310-7.

46. Wood, I. A., Visscher, P. M., and Mengersen, K. L. (2007). Classification based upon gene expression data: Bias and precision of error rates, *Bioinformatics*, Vol. 23, No. 11, 1363–1370. doi:10.1093/bioinformatics/btm117.

47. Luts, J., Ojeda, F., Van de Plas Raf, R., De Moor, B., Van Huffel, S., and Suykens, J. A. K. (2010). A tutorial on support vector machine-based methods for classification problems in chemometrics, *Analytica Chimica Acta*, Vol. 665, No. 2, 129–145. doi:10.1016/j.aca.2010.03.030.

48. Xu, Y., Zomer, S., and Brereton, R. G. (2006). Support vector machines: A recent method for classification in chemometrics, *Critical Reviews in Analytical Chemistry*, Vol. 36, Nos. 3–4, 177–188. doi:10.1080/10408340600969486.

49. Padilla-González, G. F., Aldana, J. A., and Da Costa, F. B. (2016). Chemical characterization of two morphologically related Espeletia (asteraceae) species and chemometric analysis based on essential oil components, *Revista Brasileira de Farmacognosia*, Vol. 26, No. 6, 694–700. doi:10.1016/j.bjp.2016.05.009.